THE ASTROPHYSICAL JOURNAL, 344:210–216, 1989 September 1

THE KINEMATICS OF THE SMALL MAGELLANIC CLOUD FROM ITS FIELD CARBON STARS

EDUARDO HARDY[1]
Département de Physique and Observatoire du Mont Mégantic, Université Laval
NICHOLAS B. SUNTZEFF
Cerro Tololo Inter-American Observatory, and National Optical Astronomical Observatories
AND
MARC AZZOPARDI
Observatoire de Marseille
Received 1988 September 13; accepted 1989 February 14

ABSTRACT

We present the first results of a velocity survey of the field population of carbon stars in the SMC. A total of 150 stars were observed spectroscopically in the near IR with an individual precision of ± 1.8 km s^{-1}. The carbon star population does not behave kinematically like the extreme Population I of the SMC: there is no evidence of a velocity splitting, in contradiction with the two-galaxy model of Mathewson, Ford, and Visvanathan, nor is there any evidence of rotation of the main body. In this respect carbon stars behave kinematically like the planetary nebulae system with which they share a velocity dispersion of ~ 27 km s^{-1}. Carbon stars also exhibit the same velocity dispersion as a sample of halo metal-poor giants near NGC 121. The possibility exists that carbon stars and planetary nebulae belong to a spheroidal-like system, but this is uncertain for carbon stars due to lack of better spatial coverage. There are indications of streaming motions in the wing section between the SMC and the LMC with a positive gradient of 165 ± 53 km s^{-1} degree^{-1} toward the LMC. The mass of the SMC as inferred from its velocity dispersion is near $10^9\ M_\odot$ giving a visual mass-to-light ratio near 2. The heliocentric velocity of the SMC bar is 148.3 ± 2.4 km s^{-1} (s.e.) corresponding to a galactocentric velocity of -11.3 km s^{-1}.

Subject headings: galaxies: internal motions — galaxies: Magellanic Clouds — galaxies: structure — nebulae: planetary — stars: carbon

I. INTRODUCTION

The geometrical and kinematical structure of the Magellanic Clouds is extremely complex, possibly as a result of interactions between themselves and with the Galaxy. This complexity is particularly striking in the case of the SMC where available evidence suggests considerable depth and the presence of multiple discrete structures along the line of sight (Mathewson, Ford, and Visvanathan 1986, 1988, hereafter MFV1 and MFV2, respectively). One of the most serious limitations to an understanding of the SMC structure is the scarcity of radial velocity data for its older and intermediate-age populations, since most of the known velocities belong to either supergiants, H II complexes, or diffuse H I (Torres and Carranza 1987, and references therein).

Very little velocity information is available for carbon stars in the Magellanic Clouds. These stars are ideal tracers of the stellar velocity field because they are numerous in the Clouds, are bright, and have strong absorption bands well suited for precise velocity measurement over a wide spectral range. Most importantly, because of their age interval carbon stars are very likely representative of the bulk of the field stellar population which is a few gigayears old (Hardy and Durand 1984).

In this paper we discuss the first results of a velocity survey of the SMC based on spectroscopic observations in the near IR of its field carbon stars.

[1] Visiting Astronomer, Cerro Tololo Inter-American Observatory, NOAO, operated by AURA, Inc., under contract with the National Science Foundation.

II. OBSERVATIONS

A total of 150 SMC field carbon stars (CS) were observed with the CTIO 4 m telescope in a very successful 5 night run centered around full moon in 1986 September; a second attempt in 1987 September was largely unsuccessful because of weather conditions. Most of the objects in the SMC bar were drawn from the sample described by Westerlund, Azzopardi, and Breysacher (1986), with additions from Blanco, McCarthy, and Blanco (1980); all objects in the SMC wing belonging to the latter source. The distribution of observed CS is shown in Figure 1. Notice that the distribution over the face of the galaxy is discontinuous as a result of the search patterns used by the above authors. We distinguish a SW group centered at $\alpha = 00^h48^m.6$, $\delta = -73°35'.5$ (1950), a NE group at $\alpha = 1^h01^m.7$, $\delta = -72°26'.1$, and a wing group at $\alpha = 00^h59^m.4$, $\delta = -73°20'.1$. The positions of individual stars, accurate to a few arcseconds, are listed in columns (2) and (3) of Table 1.

The observations were obtained with the 4 m RC spectrograph and Air Schmidt camera coupled to the Epitexial GEC No. 9 CCD detector used in conjunction with grating No. 380 (1200 l/mm). A 300 μm slit provided a FWHM resolution of 1.4 Å in the interval 7700–8200 Å, comprising the strong 7910 and 8100 Å CN band heads and numerous atomic and molecular features (see Seitzer and Frogel 1985). The system was remarkably stable, with no drifts larger than 0.4 pixels ever detected. The wavelength scale was determined from frequent observations of He-Ne-Ar comparison sources with checks on possible zero point drifts provided by the strong night-sky emission

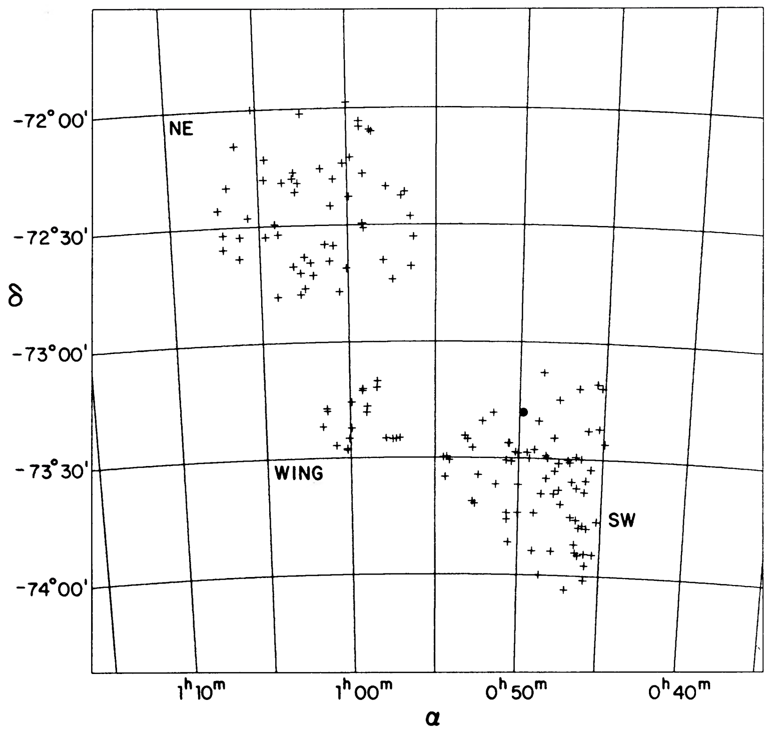

FIG. 1.—The (α, δ) distribution and grouping of observed carbon stars

spectrum. Exposure times for SMC stars averaged 3–5 minutes. The CCD spectra were trimmed, debiased, flat-fielded, sky-subtracted, wavelength-calibrated, flattened, and cross-correlated with respect to the five template carbon and CH stars, BN Mon, HD 16115, HD 13828, HD 209291, and HD 233392. This instrumental velocity was then corrected to the heliocentric system and brought to an absolute velocity system by the addition of a nightly zero-point correction. This zero point was calculated by forcing the nightly measured velocity of the templates and HD 26, V Aql, HD 52432, and HD 189711 to have the values given by Walker (1979) and McClure (1978). The external accuracy of the velocity system is estimated to be 1.5 km s^{-1} and from repeated observations of SMC program stars on different nights, we find the average error in a single observation to be 1.8 km s^{-1}, equivalent to better than 0.07 pixel. Heliocentric velocities are listed in column (4) of Table 1.

III. THE VELOCITY FIELD

We address the following questions: (1) Are there global differences between the velocity distribution of the CS and that of other measured components of the SMC such as super-

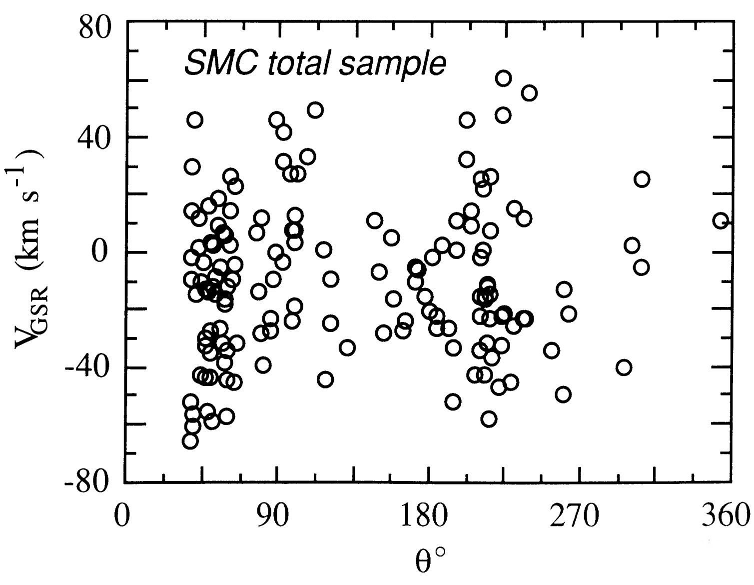

FIG. 2.—Galactocentric velocities vs. position angle for the entire sample of 150 carbon stars

giants, the neutral and ionized H, and the planetary nebulae? (2) Is the wing a dynamically distinct unit? (3) What is the mass of the SMC as derived from the velocity field of its CS?

a) *Global properties*

To test for global rotation of the carbon star population we have plotted the velocity data in Figure 2. There the vertical axis represents the observed radial velocity reduced to the Galactic System of Reference (GSR) which is free of any spurious velocity gradient introduced by rotation of our Galaxy, and which will be used throughout. The transformation from the heliocentric system was performed using a basic solar motion of 16.5 km s^{-1} and a circular motion of the LSR of 250 km s^{-1}; the resulting values for the galactocentric velocities are listed in column (5) of Table 1. The horizontal axis displays the position angle θ in the plane of the sky measured about a fiducial center located at $\alpha = 00^{\rm h}49^{\rm m}.5$ and $\delta = -73°20'$. This point is close to the center of the CS isopleths of Blanco and McCarthy (1983), corresponds closely to the position adopted for the center of the distribution of the planetary nebulae by Dopita *et al.* (1985), and lies near the position given by de Vaucouleurs and Freeman (1972) for the "optical" center of the bar. The position angle θ, which is listed in column (6) of Table 1, is zero to the north and increases to the east, as usual.

Figure 2 is analogous to Figure 7 of Freeman, Illingworth, and Oemler (1983) which was used to obtain a rotation solution for the system of older clusters in the LMC. As discussed by them, the $V_{\rm GSR}$ versus θ diagram can be used to obtain a least-square fit of the function

$$V(\theta) = V_m\{[\tan(\theta + \theta_0) \sec i]^2 + 1\}^{-1/2} + V_0 \qquad (1)$$

in order to obtain the various parameters: θ_0 is the line of nodes, V_m is the amplitude of the rotation solution, V_0 is the systemic velocity, and i is the inclination. Figure 2 shows no systematic trend, however, the observed velocities being clearly independent of position angle. Thus, no structural information

TABLE 1

SMC Data

Star	α (1950)	δ (1950)	V(Hel.) (km s^{-1})	V(GSR) (km s^{-1})	θ (deg)	Star	α (1950)	δ (1950)	V(Hel.) (km s^{-1})	V(GSR) (km s^{-1})	θ (deg)
SW						SW					
1...	0 44 56	-73 25 57	124.2	-34.5	253.5	39...	0 48 17	-73 29 49	136.6	-22.9	215.9
2...	0 45 11	-73 11 33	118.1	-40.0	295.8	40...	0 48 18	-73 29 47	144.7	-14.8	215.9
3...	0 45 15	-73 46 02	112.5	-47.1	221.6	41...	0 48 21	-73 35 08	116.6	-43.1	207.8
4...	0 45 17	-73 22 05	137.0	-21.6	263.0	42...	0 48 23	-73 29 14	101.7	-57.8	215.5
5...	0 45 27	-73 54 30	128.3	-31.7	214.8	43...	0 48 36	-73 07 45	169.8	11.2	353.5
6...	0 45 28	-73 10 30	160.7	2.6	300.8	44...	0 48 38	-73 39 06	192.0	32.1	201.7
7...	0 45 41	-73 32 41	171.1	12.0	235.7	45...	0 48 40	-73 59 53	161.6	0.8	196.4
8...	0 45 51	-73 47 48	122.6	-37.2	216.9	46...	0 48 51	-73 20 17	109.6	-49.6	260.7
9...	0 45 53	-73 57 17	160.8	0.6	211.2	47...	0 49 02	-73 44 01	170.8	10.6	196.0
10...	0 45 54	-73 22 37	146.1	-12.6	260.0	48...	0 49 04	-73 27 42	168.8	9.3	203.7
11...	0 45 55	-74 01 06	144.6	-15.7	209.5	49...	0 49 06	-73 53 43	108.4	-52.2	194.4
12...	0 45 57	-73 54 20	145.0	-15.1	212.4	50...	0 49 22	-73 29 59	126.7	-33.0	194.5
13...	0 45 58	-73 35 35	114.1	-45.2	229.1	51...	0 49 30	-73 28 28	133.4	-26.2	191.8
14...	0 46 02	-73 38 32	138.3	-21.1	224.6	52...	0 50 00	-73 36 51	138.1	-22.0	184.6
15...	0 46 06	-73 47 07	167.7	7.9	216.1	53...	0 50 01	-73 43 59	162.8	2.4	186.7
16...	0 46 16	-73 30 01	135.7	-23.4	237.3	54...	0 50 02	-73 28 39	144.4	-15.3	176.9
17...	0 46 19	-73 47 40	148.1	-11.7	214.5	55...	0 50 12	-73 28 26	154.1	-5.7	172.1
18...	0 46 20	-73 54 45	137.7	-22.4	210.3	56...	0 50 26	-73 30 47	155.0	-4.9	171.0
19...	0 46 30	-73 54 06	185.8	25.7	209.8	57...	0 50 26	-73 30 50	149.6	-10.3	171.3
20...	0 46 30	-73 11 47	153.2	-5.2	305.3	58...	0 50 34	-73 26 07	131.7	-28.0	152.4
21...	0 46 30	-73 37 32	126.9	-32.6	222.7	59...	0 50 34	-73 51 37	134.4	-26.4	183.9
22...	0 46 30	-73 45 39	148.6	-11.2	214.8	60...	0 50 38	-73 26 03	152.8	-6.9	150.4
23...	0 46 34	-73 51 58	158.6	-1.5	210.4	61...	0 50 40	-73 45 43	159.1	-1.5	180.9
24...	0 46 35	-73 29 30	135.8	-23.3	236.1	62...	0 50 42	-73 44 07	140.3	-20.2	180.1
25...	0 46 48	-73 35 57	137.5	-21.9	222.4	63...	0 50 45	-73 30 35	132.8	-27.1	164.2
26...	0 46 50	-73 44 57	143.8	-16.0	213.2	64...	0 51 21	-73 36 50	136.3	-24.0	165.8
27...	0 46 57	-73 30 56	174.6	15.3	229.7	65...	0 51 32	-73 18 13	171.6	12.0	80.2
28...	0 47 04	-73 30 21	133.4	-25.9	229.9	66...	0 52 11	-73 20 25	191.0	31.2	93.0
29...	0 47 04	-74 03 36	175.1	14.5	203.6	67...	0 52 24	-73 34 25	171.3	10.9	147.6
30...	0 47 27	-73 41 43	181.9	22.1	211.0	68...	0 52 37	-73 41 45	144.1	-16.7	158.7
31...	0 47 35	-73 38 05	117.3	-42.4	213.0	69...	0 52 45	-73 27 20	135.2	-25.0	121.5
32...	0 47 36	-73 31 13	206.8	47.4	222.5	70...	0 52 45	-73 41 11	166.0	5.2	156.5
33...	0 47 37	-73 31 12	220.2	60.8	222.3	71...	0 53 03	-73 25 07	210.0	49.8	110.7
34...	0 47 39	-73 14 44	184.4	25.7	305.9	72...	0 53 13	-73 24 14	193.6	33.5	106.5
35...	0 47 50	-73 33 13	185.7	26.2	216.2	73...	0 54 08	-73 30 34	150.7	-9.9	121.5
36...	0 47 52	-73 39 05	125.7	-34.1	209.6	74...	0 54 18	-73 29 40	116.2	-44.4	118.2
37...	0 47 54	-73 24 38	214.7	55.5	238.3	75...	0 54 24	-73 34 55	127.6	-33.2	130.6
38...	0 47 56	-73 53 46	206.4	46.0	201.8	76...	0 54 29	-73 29 48	161.5	0.9	117.6

can be derived from Figure 2 other than the important conclusion that there is no overall rotation of the carbon star population.

In order to compare our carbon star data with results derived in the literature for the Population I velocity indicators we have adopted projections of our velocity data along the principal axes as shown in Figure 3. The adopted major axis follows closely the direction of maximum light and maximum H I density (Torres and Carranza 1987; Loiseau and Bajaja 1981). Our results are not strongly dependent on the precise orientation of the axes or on the exact position of the adopted SMC center. In the first panel on Figure 3 we show the major axis projection (P. A. = 56°) for the entire data sample, in the second the minor axis projection (P. A. = 146°) also for the entire data sample, and in the third the minor axis projection for the wing subsample alone. Table 2 displays the relevant statistical parameters for the two groups of CS listed under column (1), with populations N (col. [2]). The Bar includes the SW and NE regions. Columns (3)–(5) display the coefficients of the least-mean-square fit of the radial velocity data to an expression of the form

$$V_{\rm GSR} = S \times R + I \,, \tag{2}$$

where R is the projected (major or minor axis) distance of the star from the adopted fiducial center. The velocity gradients S are defined positive if the velocity increases toward the SW (major axis) or toward the SE (minor axis). The errors quoted in columns (7), (8), and (9) are the standard error of the mean. Finally, column (10) contains the radial rms velocity dispersion $\langle V^2 \rangle^{1/2}$ together with the statistical error due to the finite sample size, which was computed from the $(2/N)^{1/2}$ scaling law of the velocity variance $\langle V^2 \rangle$ (Armandroff and da Costa 1986).

TABLE 1—*Continued*

Star	α (1950)	δ (1950)	V(Hel.) (km s^{-1})	V(GSR) (km s^{-1})	θ (deg)	Star	α (1950)	δ (1950)	V(Hel.) (km s^{-1})	V(GSR) (km s^{-1})	θ (deg)
Wing						Wing					
1...	0 57 05	-73 24 48	173.4	12.5	99.0	11...	0 59 54	-73 15 31	133.4	-27.7	84.7
2...	0 57 18	-73 25 00	142.5	-18.5	99.2	12...	0 59 55	-73 22 11	157.8	-3.5	93.1
3...	0 57 30	-73 25 06	164.5	3.5	99.0	13...	1 00 04	-73 24 53	189.1	27.6	96.6
4...	0 57 54	-73 24 53	136.8	-24.3	98.3	14...	1 00 11	-73 27 35	169.5	7.9	100.0
5...	0 58 24	-73 10 04	167.3	6.7	76.5	15...	1 00 11	-73 27 55	188.5	26.9	100.4
6...	0 58 25	-73 11 42	147.1	-13.5	78.7	16...	1 00 50	-73 26 43	168.9	7.2	98.4
7...	0 58 60	-73 16 37	137.8	-23.1	85.6	17...	1 01 21	-73 17 48	207.8	46.4	87.8
8...	0 59 03	-73 18 09	160.9	-0.1	87.8	18...	1 01 22	-73 17 07	151.7	-9.7	87.0
9...	0 59 15	-73 12 00	132.7	-28.1	79.9	19...	1 01 37	-73 21 47	203.2	41.5	92.2
10...	0 59 16	-73 12 31	121.1	-39.7	80.6						
NE						NE					
1...	0 56 16	-72 33 03	144.1	-14.5	40.6	29...	1 02 08	-72 39 36	142.0	-18.1	58.2
2...	0 56 24	-72 40 37	155.8	-3.2	44.8	30...	1 02 28	-72 46 12	151.0	-9.4	62.5
3...	0 56 27	-72 27 50	102.3	-56.2	39.0	31...	1 02 29	-72 38 06	144.0	-16.1	58.0
4...	0 56 46	-72 21 29	105.7	-52.6	37.7	32...	1 02 33	-72 01 19	115.7	-42.9	44.3
5...	0 56 58	-72 22 32	148.9	-9.4	38.6	33...	1 02 42	-72 42 14	174.5	14.2	60.6
6...	0 57 28	-72 44 03	115.5	-43.8	50.1	34...	1 02 43	-72 47 43	115.5	-45.0	63.8
7...	0 57 50	-72 20 09	204.4	46.0	40.1	35...	1 02 47	-72 19 06	131.7	-27.7	50.3
8...	0 58 00	-72 39 06	175.1	15.9	48.8	36...	1 02 56	-72 21 22	161.7	2.2	51.4
9...	0 58 38	-72 06 03	92.4	-65.6	37.8	37...	1 03 00	-72 16 22	162.7	3.4	49.7
10...	0 58 45	-72 05 34	187.7	29.7	38.0	38...	1 03 05	-72 17 55	100.6	-58.8	50.4
11...	0 59 07	-72 30 48	145.5	-13.6	47.5	39...	1 03 07	-72 40 27	148.0	-12.3	60.3
12...	0 59 08	-72 16 51	159.7	1.2	42.2	40...	1 03 40	-72 18 55	147.8	-11.8	51.7
13...	0 59 11	-72 29 34	126.8	-32.3	47.1	41...	1 03 57	-72 32 13	166.5	6.3	57.5
14...	0 59 18	-72 04 48	97.7	-60.4	39.0	42...	1 04 03	-72 48 12	129.0	-31.8	66.0
15...	0 59 19	-72 03 24	172.6	14.6	38.6	43...	1 04 07	-72 29 33	166.8	6.7	56.7
16...	0 59 49	-72 12 41	170.5	12.0	42.3	44...	1 04 36	-72 12 56	162.3	2.8	51.1
17...	0 59 55	-72 22 43	128.8	-30.1	46.0	45...	1 04 39	-72 32 45	121.6	-38.7	58.9
18...	0 59 59	-71 58 30	156.2	-1.8	38.8	46...	1 04 40	-72 18 03	145.4	-14.3	53.0
19...	1 00 06	-72 41 05	133.2	-26.5	55.0	47...	1 05 16	-71 59 57	103.2	-55.9	48.3
20...	1 00 15	-72 14 11	148.5	-10.2	43.7	48...	1 05 37	-72 27 43	166.6	6.3	58.1
21...	1 00 30	-72 47 08	115.5	-44.6	59.6	49...	1 06 07	-72 32 36	162.7	2.1	60.8
22...	1 00 48	-72 18 10	115.6	-43.3	46.2	50...	1 06 10	-72 38 07	156.4	-4.4	63.4
23...	1 00 50	-72 35 18	178.5	18.9	53.4	51...	1 06 14	-72 09 13	150.9	-8.8	52.3
24...	1 00 57	-72 25 02	124.5	-34.8	49.1	52...	1 06 45	-72 19 48	128.1	-32.1	56.6
25...	1 01 03	-72 39 14	154.2	-5.6	56.0	53...	1 07 03	-72 31 57	187.1	26.3	61.7
26...	1 01 18	-72 34 56	168.6	8.9	54.2	54...	1 07 05	-72 35 38	184.0	23.1	63.4
27...	1 01 29	-72 15 29	146.0	-13.0	46.6	55...	1 07 17	-72 25 34	103.1	-57.5	59.4
28...	1 01 60	-72 42 49	126.3	-33.9	59.7						

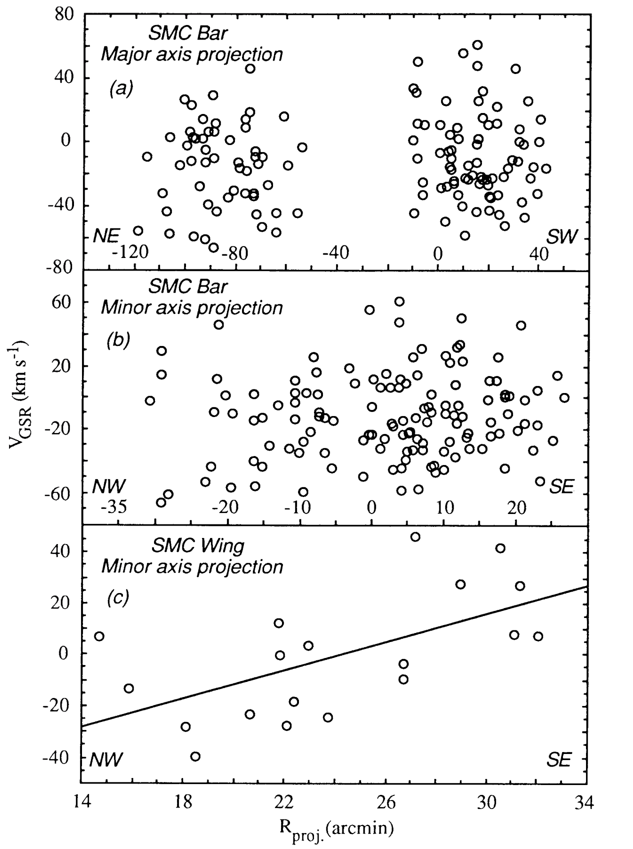

FIG. 3.—Projection of the Bar velocity data sample along the major axis at P. A. = 56° (*a*), along the minor axis (*b*), and projection of the wing velocity data (19 stars) along the minor axis (*c*). The least-square linear fit to the wing data is shown.

The value of $26.8^{+1.6}_{-1.7}$ km s^{-1} given in column (10) for the SMC Bar is probably among the best determined optical velocity dispersions for any external galaxy.

A common characteristic of all young velocity indicators, H I, H II, supergiant stars, is a velocity gradient of $\sim$10–30 km s^{-1} increasing in the SW–NE direction along a $\sim$60° position angle which follows closely the major axis of the bar (Torres and Carranza 1987, their Fig. 5 and references therein), and which is also closely oriented in the direction of the maximum *distance* gradient as defined by the Cepheids (Caldwell and Coulson 1986, their Fig. 15; see also MFV2). This velocity gradient is often interpreted as indicating rotation of the main body (de Vaucouleurs and Freeman 1972, and references therein; but see also MFV1, 2). Inspection of Figure 3 and of the slopes and standard errors in Table 2 indicate the absence of radial velocity gradients for the CS along either the major or the minor axis of the bar; the only statistically significant gradient detected in our data being along the minor axis of the Wing, which will be discussed later. Testing for kinematical effects involving CH stars within our sample, which would then isolate an older population, is of obvious interest (Hartwick and Cowley 1988), but we don't have enough spectral information at our disposal to identify CH stars and examine the question at the present time. Using the available information we have tested for the possibility that subpopulations of CS in the Bar may exhibit velocity gradients by binning the data according to the value of $C_2(d)$, the depth of the C_2 Swan band at 5165 Å (or the strongly correlated color index $m_3 - m_1$), as defined and tabulated for the 103 stars in common by Westerlund, Azzopardi, and Breysacher (1986). Again, no statistically significant gradients were found. Notice that a gradient of -20 km s^{-1} deg^{-1} across the bar, compatible with the mean value observed for the young population (Torres and Carranza 1987, their Fig. 5), is 8.5 standard errors away from our global value of 3.2 ± 2.7 from Table 2.

These negative results are somewhat puzzling and indicate that the carbon star population is kinematically very different from the younger population defining the SMC rotation curve. But recent studies of the kinematics of 44 SMC planetary nebulae by Dopita *et al.* (1985) also indicate lack of organized rotation as shown in their Figure 4. Furthermore, our results of Table 2 (and Fig. 4, below) indicate a velocity dispersion essentially independent of position and virtually identical to the value of $25.3^{+2.6}_{-2.9}$ km s^{-1} obtained by Dopita *et al.* (1985). They interpret the PN population surveyed over a larger angular distance than our carbon stars, but with a smaller sample, as being part of a spheroidal system on the basis of a fit to its spatial distribution. It is also interesting to note that from their Tables 3 and 4 a value 134.2 ± 3.8 km s^{-1} (s.e.) for the mean LSR radial velocity of 44 PN obtains which is identical, within the combined standard error of 4.5 km s^{-1}, to our value of 139.7 ± 2.4 km s^{-1} (s.e.) derived from 131 CS projected on the bar.

Next we ask whether our data are consistent with the predictions of the MFV1, 2 model which assumes two separated fragments over much of the SMC angular size. In their picture the two fragments differ in radial velocity by $\sim$40 km s^{-1}, with the low-velocity component (the SMC Remnant) being in front of the high-velocity component (the Mini Magellanic Cloud) and extending further to the NE. Figure 4 presents radial velocity histograms for three groupings of Bar CS. Our data show no evidence of the predicted bimodal velocity distribution for any of them, a result also in agreement with the PN data of Dopita *et al.* (1985).

In order to further compare the velocity distributions for the NE and SW sections we have performed a two-tailed Kolgomorov-Smirnov test, which has the advantage of being independent of any particular binning of the data, and

TABLE 2

VELOCITY DATA FOR CARBON STARS IN SMC

		MAJOR AXIS		MINOR AXIS					
IDENTIFICATION (1)	N (stars) (2)	S (km s^{-1} deg^{-1}) (3)	I (km s^{-1}) (4)	S (km s^{-1} deg^{-1}) (5)	I (km s^{-1}) (6)	$\langle V_{Hel.} \rangle$ (km s^{-1}) (7)	$\langle V_{LSR} \rangle$ (km s^{-1}) (8)	$\langle V_{GS} \rangle$ (km s^{-1}) (9)	$\langle V^2 \rangle^{1/2}$ (km s^{-1}) (10)
Bar	131	3.20 ± 2.74	-9.86	13.31 ± 10.31	-11.81	148.3 ± 2.4	139.7 ± 2.4	-11.3 ± 2.4	$26.8^{+1.6}_{-1.7}$
Wing	19	-9.26 ± 52.91	-5.84	165.09 ± 53.08	-66.58	160.7 ± 5.6	152.0 ± 5.6	-0.4 ± 5.6	$24.2^{+3.7}_{-4.3}$

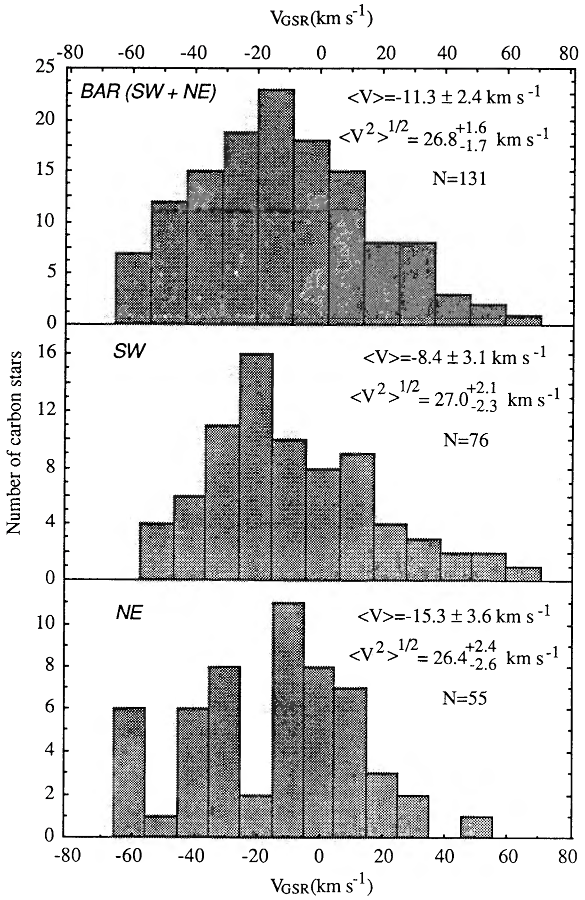

FIG. 4.—Radial velocity histograms for the SMC Bar and sections of it. Mean galactocentric velocities and velocity dispersions are indicated.

obtained a significance level of 0.21. The null hypothesis (that the two samples were taken from the same parent population) can therefore be accepted with a high degree of confidence.

A number of interpretations of our results come to mind which are consistent with the lack of observable organized rotation. First we may consider the possibility that the CS population does rotate as a whole but on a plane normal to the line of sight and inclined with respect to the younger population. Second, the CS population may belong almost exclusively to the SMCR (as defined by MVF), with which it shares a common LSR radial velocity of ~ 140 km s^{-1}. Finally, it may be argued that the SMC carbon stars belong to a *spheroidal* population, much as the planetary nebulae seem to do, with nearly null total angular momentum. The SMC would then consist of a younger population, perhaps a two-armed galaxy with a central bar seen edge on, as in Caldwell and Coulson (1986), or even two detached fragments as in MFV1, 2 embedded on a spheroidal system, including CS and PN, which doesn't show evidence for collisional disruption.

The first possibility is unlikely because it would require a fortuitous alignment of the CS disk with respect to the rest of the SMC at precisely the required angle. The second alternative is possible but it demands that all (or at least most) CS be concentrated on one of the two SMC components, whereas all younger objects are well represented in both the MMC and the SMCR. We call attention to the fact that we found no evidence of spatial selection for any subsample chosen according to its $C_2(d)$ index. It would then also have required that the stripping process acted upon only the young population without affecting the older disk. Finally, the hypothesis that the CS form a spheroidal population is attractive because it naturally explains the observations without invoking complex geometry and because it fits well with the observations of at least another stellar population, the PN (Dopita *et al.* 1985). Is there, on the other hand, any independent evidence that the CS constitute a spheroidal-like halo population? The spatial distribution of CS over the face of the SMC has been mapped by Blanco and McCarthy (1983) and more recently by Rebeirot *et al.* (1987). But these data suffer from sampling inhomogeneities or completeness problems, or both, and only when properly corrected will they be able to provide a test through a fit to a specific projected density distribution. A kinematical result suggesting that the CS sample studied here behave in at least one respect like the SMC halo population does, however, exist. Suntzeff *et al.* (1986) found a halo velocity dispersion of 24.2 km s^{-1} based on observations of 12 metal-poor giants near NGC 121; a value identical within the errors to that found here from CS. Whether the SMC metal poor halo population itself forms a spheroidal system remains unknown.

b) *Streaming Motions in the Wing?*

The only significant velocity gradient detected in our data is shown in Figure 3*c* which indicates a velocity gradient of 165 ± 53 km s^{-1} deg^{-1} increasing in the NW–SE sense in the direction of the LMC. Unless the wing section of the SMC is a separated entity with a rotational motion of its own, the tentative conclusion is that we are seeing streaming motions along the LMC–SMC bridge which attaches itself to the SMC through the wing region. The presence of an H I ridge extending from the wing has been known for some time (Loiseau and Bajaja 1981). More recently, Irwin, Kunkel, and Demers (1985) have reported the discovery of a stellar population with an age of $\sim 10^8$ yr in the H I bridge between the Clouds, but no extensive survey of CS has been conducted so far in that region.

We may speculate that the velocity perturbation produced by a close encounter with the LMC (Murai and Fujimoto 1980) is more easily detected as one moves away from the SMC main mass distribution. But a much larger sample of CS velocities extending from the bar center, which itself was not included in this investigation, to further distances along the wing are necessary to test the reality of a possible stellar stream as well as any dynamical model of the SMC.

c) *Mass of the SMC*

The lack of any significant rotational support for the CS population suggests that the total mass M of the SMC can be estimated by methods employing the velocity dispersion of its carbon stars (~ 27 km s^{-1} from Table 2). These methods, however, depend strongly on the assumed mass distribution model (Binney and Tremaine 1987; Bahcall and Tremaine 1981, pp. 213–214). Adoption of the variation of the virial theorem used by Dopita *et al.* (1987) yields their result, $M = 9 \times 10^8 M_\odot$, since we have measured essentially the same value of the velocity dispersion. The projected mass distribition method of Bahcall and Tremaine (1981) gives $M = 0.8\,\mu \times 10^9 M_\odot$, where the geometrical factor μ takes the value $\frac{2}{3}$ for circular stellar orbits, 1 for an isotropic velocity distribution, and 2 for linear orbits. Pending a more refined mass distribution model, which would require considerably more data, all we can conclude on the basis of our observations is that the mass of the SMC contained within the volume sampled by the carbon stars is very near 10^9 $M_\odot$. Adopting a total absolute visual luminosity $M_V = -16.9$ from the photometry provided by Bothun and Thompson (1988) and the distance modulus of Walker and Mack (1988) we obtain a visual mass-to-light ratio near 2 which is close to the value obtained in the solar neighborhood. This value is considerably lower than those obtained for the Local Group dwarf spheroidal galaxies using the velocity dispersion of carbon stars and K giants (Aaronson and Olszewski 1987).

IV. CONCLUSIONS

A study of the radial velocities of field carbon stars in the SMC provides the following information on its structure. (1) The kinematical behavior of the carbon star population is different from that of the younger populations. The lack of significant rotation may indicate the presence of a spheroidal population, of which the planetary nebulae may also be part; a result that can only be substantiated by the kinematical and spatial study of a larger sample of CS. It should be added here that, although unlikely on the basis of the present data since the slope of the minor axis rotation curve does not change significantly with the inclusion of the Wing data, a slight spindle-like rotation of the SMC about the major axis can only be definitively excluded by the study of a larger more continuous sample, including the center and further-away portions of the SMC. Also, deviations from a Gaussian shape may exist in Figure 4, although a larger sample would be required to test for the precise shape of the velocity distribution. (2) The section of the SMC wing, studied here with only 19 members, exhibits a velocity gradient which (if it is not a sample effect) is suggestive of motions toward the LMC, possibly along the known bridge between these galaxies. (3) There are no indications of the bimodal velocity distribution predicted by the two-galaxy model of MFV1, 2 although a larger sample of carbon stars may uncover more subtle effects. (4) Finally, a study of the velocity dispersion of the CS population suggests a total mass for the SMC near 10^9 $M_\odot$, with considerable uncertainties resulting from a lack of a well understood mass-distribution model. The derived visual mass-to-light ratio is near 2. Study of a larger sample of SMC field and cluster carbon stars, now underway, will help refine the ideas and results presented here.

E. H. acknowledges support by NSERC-Canada.

REFERENCES

Aaronson, M., and Olszewski, E. W. 1987, in *IAU Symposium 117, Dark Matter in the Universe*, ed. J. Kormendy and G. R. Knapp (Dordrecht: Reidel), p. 153.
Armandroff, T. E., and Da Costa, G. S. 1986, *A.J.*, **92**, 777.
Bahcall, J. N., and Tremaine, S. 1981, *Ap. J.*, **244**, 805.
Binney, J., and Tremaine, S. 1987, *Galactic Dynamics*, (Princeton: Princeton University Press).
Blanco, V. M., and McCarthy, M. F. 1983, *A.J.*, **88**, 1442.
Blanco, V. M., McCarthy, M. F., and Blanco, B. M. 1980, *Ap. J.*, **242**, 938.
Bothun, G. D., and Thompson, I. B. 1988, *A.J.*, **96**, 877.
Caldwell, J. A. R., and Coulson, I. M. 1986, *M.N.R.A.S.*, **218**, 223.
de Vaucouleurs, G., and Freeman, K. C. 1972, *Vistas Astro.*, **14**, 163.
Dopita, M. A., Ford, H. C., Lawrence, C. J., and Webster, B. L. 1985, *Ap. J.*, **296**, 390.
Freeman, K. C., Illingworth, G., and Oemler, A. 1983, *Ap. J.*, **272**, 488.
Hardy, E., and Durand, D. 1984, *Ap. J.*, **279**, 567.
Hartwick, F. D. A., and Cowley, A. P. 1988, *Ap. J.*, **334**, 135.
Irwin, M. J., Kunkel, W. E., and Demers, S. 1985, *Nature*, **318**, 160.
Loiseau, N., and Bajaja, E. 1981, *Rev. Mexicana Astr. Ap.*, **6**, 55.
Mathewson, D. S., Ford, V. L., and Visvanathan, N. 1986, *Ap. J.*, **301**, 664 (MVF1).
———. 1988, *Ap. J.*, **333**, 617 (MFV2).
McClure, R. 1987, Private communication.
Murai, T., and Fujimoto, M. 1980, *Pub. Astr. Soc. Japan*, **32**, 581.
Rebeirot, E., Azzopardi, M., Breysacher, J., and Westerlund, B. E. 1987, in *Proc. ESO Conf. and Workshop 27*, ed. M. Azzopardi and F. Matteucci (Garching: ESO), p. 263.
Seitzer, P., and Frogel, J. A. 1985, *A.J.*, **90**, 1796.
Suntzeff, N. B., Friel, E., Klemola, A., Kraft, R. P., and Graham, J. A. 1986, *A.J.*, **91**, 275.
Torres, G., and Carranza, G. C. 1987, *M.N.R.A.S.*, **226**, 513.
Walker, A.R. 1979, *SAAO Circ.*, Vol. **1**, No. 4, p. 112.
Walker, A. R., and Mack, P. 1988, *A.J.*, **96**, 872.
Westerlund, B. E., Azzopardi, M., and Breysacher, J. 1986, *Astr. Ap. Suppl.*, **65**, 79.

M. Azzopardi: Observatoire de Marseille, 2 Place Le Verrier, 13249 Marseille, Cedex 4, France

E. Hardy: Département de Physique, Université Laval, Sainte-Foy, Québec, Canada, G1K 7P4

N. B. Suntzeff: Cerro Tololo Inter-American Observatory, Casilla 603, La Serena, Chile